

Melanoma Detection Using Machine Learning



Author

Kashan Zafar

NUST00000207013

Supervisor

Dr Omer Gilani

DEPARTMENT OF BIOMEDICAL ENGINEERING

SCHOOL OF MECHANICAL & MANUFACTURING ENGINEERING

NATIONAL UNIVERSITY OF SCIENCES AND TECHNOLOGY

ISLAMABAD

2019

Melanoma Detection Using Machine Learning

By

Kashan Zafar

00000207013

A thesis submitted in partial fulfillment of the requirements for the degree of
MS Biomedical Engineering

Thesis Supervisor:

Dr Omer Gilani

Thesis Supervisor's Signature: _____

DEPARTMENT OF BIOMEDICAL ENGINEERING
SCHOOL OF MECHANICAL & MANUFACTURING ENGINEERING
NATIONAL UNIVERSITY OF SCIENCES AND TECHNOLOGY,
ISLAMABAD

December 2019

THESIS ACCEPTANCE CERTIFICATE

It is certified that final copy of MS thesis written by KASHAN ZAFAR Registration No. 00000207013 of SMME has been vetted by undersigned, found complete in all respects as per NUST Statutes / Regulations, is free of plagiarism, errors, and mistakes and is accepted as partial fulfillment for award of MS/MPhil degree. It is further certified that necessary amendments as pointed out by GEC members of the scholar have also been incorporated in the said dissertation

Signature: _____

Name of Supervisor: _____

Date: _____

Signature (HOD): _____

Date: _____

Countersign by

Signature (Dean/Principal): _____

Date: _____

MASTER THESIS WORK

We hereby recommend that the dissertation prepared under our supervision by **Kashan Zafar** (Registration No. **00000207013**), Titled: **Melanoma Detection Using Machine Learning** be accepted in partial fulfillment of the requirements for the award of MS degree. Grade _____

Examination Committee Members

1. Name: Dr. Asim Waris Signature: _____

2. Name: Dr. Umer Ansari Signature: _____

Supervisor's name: Dr. Omer Gilani Signature: _____

Date: _____

Head of Department

Date

COUNTERSIGNED

Date: _____ Dean/Principal

Declaration

I certify that this research work titled “*Melanoma Detection using machine learning*” is my own work. The work has not been presented elsewhere for assessment. The material that has been used from other sources has been properly acknowledged / referred.

Kashan Zafar

MS BME 00000207013

Plagiarism Certificate (Turnitin Report)

This thesis has been checked for Plagiarism. Turnitin report endorsed by Supervisor is attached.

Kashan Zafar

00000207013

Thesis Supervisor:

Dr. Omer Gilani

Copyright Statement

- Copyright in text of this thesis rests with the student author. Copies (by any process) either in full, or of extracts, may be made only in accordance with instructions given by the author and lodged in the Library of NUST School of Mechanical & Manufacturing Engineering (SMME). Details may be obtained by the Librarian. This page must form part of any such copies made. Further copies (by any process) may not be made without the permission (in writing) of the author.
- The ownership of any intellectual property rights which may be described in this thesis is vested in NUST School of Mechanical & Manufacturing Engineering, subject to any prior agreement to the contrary, and may not be made available for use by third parties without the written permission of the SMME, which will prescribe the terms and conditions of any such agreement.
- Further information on the conditions under which disclosures and exploitation may take place is available from the Library of NUST School of Mechanical & Manufacturing Engineering, Islamabad.

Acknowledgements

I am thankful to my Creator Allah Subhana-Watala to have guided me throughout this work at every step and for every new thought which You set up in my mind to improve it. Indeed I could have done nothing without Your priceless help and guidance. Whosoever helped me throughout the course of my thesis, whether my parents or any other individual was Your will, so indeed none be worthy of praise but You.

I am profusely thankful to my beloved parents who raised me when I was not capable of walking and continued to support me throughout in every department of my life.

I would also like to express special thanks to my supervisor Dr. Omer Gilani and GEC members Dr. Asim Waris and Dr. Umer Ansari for their help throughout my thesis.

I am highly grateful to my friends Ali Ahmad, Mahnoor Ali, Naveed Ahmed, Anum Hamid and Zunaira Qureshi for their valuable help and support throughout my thesis.

Finally, I would like to express my gratitude to all the individuals who have rendered valuable assistance to my study.

*Dedicated to my exceptional parents and supervisor, whose
tremendous support and cooperation led me to this wonderful
accomplishment.*

Table of Contents

MASTER THESIS WORK	ii
Declaration	iii
Plagiarism Certificate (Turnitin Report)	iv
Copyright Statement	v
Acknowledgements	vi
Table of Contents	viii
List of Figures	xi
List of Tables	xii
ABSTRACT	xiii
CHAPTER 1: Introduction	3
Background of the Problem	3
Statement of Purpose	4
Statistics of Melanoma	4
Objectives	5
Designing of Algorithm.....	5
Model Testing	6
CHAPTER 2: Literature Review	8
Imaging Techniques	8
Epiluminescence Microscopy (ELM).....	9
Pre-Processing Techniques.....	10
Image Segmentation	11
Artificial Intelligence Based Methods	12
Active Contour Based Segmentation.....	13

CHAPTER 3: Methodology	16
Methodology.....	16
Dataset	16
Pre-Processing	16
Image Scaling	17
Hair Removal.....	17
Image Inpainting.....	18
Image Standardization and Normalization	19
Rotation	20
Median Filtering	20
Network Architecture	21
Encoder Decoder based Architectures.....	21
ResNet 50	21
U-Net	22
Sigmoid Layer	23
Hyperparameters.....	24
Optimizers	24
Gradient Descent	24
Adam Optimizer	26
Loss Function	27
Binary Cross-entropy.....	27
Evaluation Metrics.....	27
Jaccard Index:	29
Dice Coefficient.....	30
CHAPTER 4: Results	32

Skin Lesion Segmentation	32
Pre-Processing	32
Hair Removal Algorithm	32
BlackHat Filter	32
Rotation	35
Network Architecture	37
ResNet 50	37
U-Net	39
Hyperparameters.....	41
Segmentation Results	41
Training Accuracy Graph	43
Training Loss Graph.....	44
Receiver Operator Characteristics (ROC) Curve	45
Results Benchmarking on ISIC 2017 Dataset	46
Results Benchmarking on PH ² Dataset	47
CHAPTER 5: Conclusion and Discussions	49
Future Aspects	49
REFERENCES.....	51

List of Figures

Figure 1. Dermatoscope	10
Figure 2. Distribution of methods according to applied principle	14
Figure 3. Image Inpainting pixel plane	19
Figure 4. Image Data Distribution	20
Figure 5. Residual Block of ResNet 50.....	22
Figure 6. 3-Channel Convolution.....	22
Figure 7. Sigmoid Function Graph	23
Figure 8. Gradient Descent	25
Figure 9. Comparison of Adam with other optimizers	26
Figure 10. Log Loss	27
Figure 11. Jaccard Index Overlap	30
Figure 12. Dataset Images.....	32
Figure 13. 17×17 Cross shaped Structuring Element.....	33
Figure 14. Hair Removal Algorithm.....	34
Figure 15. Thresholded Binary Mask	34
Figure 16. Final inpainted image.	35
Figure 17. Image Augmentation	36
Figure 18. Training Block Diagram.....	37
Figure 19. Schematic diagram representing UResNet-50.....	39
Figure 20. Model Accuracy Graph	43
Figure 21. Model Loss graph	44
Figure 22. Receiver Operator Characterization Curve.....	45

List of Tables

Table 1. Imaging Techniques	9
Table 2. State of the art pre-processing methods	11
Table 3. Segmentation Methods.....	12
Table 4. ISIC Dataset Distribution.....	16
Table 5. Encoder Architecture	38
Table 6. Decoder Architecture	40
Table 7. Hyperparameters	41
Table 8. Comparison of actual and predicted labels.	42
Table 9. Results Benchmarking with top ranked participant on leaderboard (ISIC 2017 Dataset)	46
Table 10. Results Benchmarking with existing architectures on PH ² dataset.....	47

ABSTRACT

Clinical treatment of skin lesion is primarily dependent on timely detection and delimitation of lesion boundaries for accurate cancerous region localization. Prevalence rate of skin cancer is on the higher side, especially that of Melanoma, which is aggressive in nature due to its high metastasis rate. Therefore, timely diagnosis is critical for its treatment before the onset of malignancy. To address this problem, medical imaging is used for analysis and segmentation of lesion boundaries from dermoscopic images. Various methods have been used ranging from visual inspection to the textural analysis of the images. However, accuracy of these methods is low for proper clinical treatment because of the sensitivity involved in surgical procedures or drug application. This presents an opportunity to develop an automated model with good accuracy so that it may be used in a clinical setting. This paper proposes an automated method for segmenting lesion boundaries that combines two architectures; the U-Net and the Res-Net, collectively called as Res-UNet. Moreover, we also use image inpainting for hair removal which improves the segmentation results significantly. We trained our model on the ISIC 2017 dataset and validated it on the ISIC 2017 test set and the PH2 dataset. Our proposed model attained Jaccard Index of 0.772 on the ISIC 2017 test set and 0.854 on the PH2 dataset, which are comparable results to the current available state of the art techniques.

Key Words: Convolutional Neural Network

Introduction

CHAPTER 1: Introduction

Background of the Problem

Skin is the largest organ of human body. It shields internal parts of our body. Skin produces Vitamin D in our body and keeps body parts intact and shaped. Skin guards our body from ultraviolet rays coming from sun. With variations in external environment it keeps body's temperature constant [1].

In the recent times, skin cancer has been increasing to a great extent in addition to reported cases of patient deaths [2]. Frequency of skin cancer doubles after every 20 years [3]. Skin cancer is divided into three main groups; Basel cell skin cancers (Basel cell carcinomas) Squamous cell skin cancers (Squamous cell carcinomas) and melanomas. Basel cell skin cancer and Squamous cell skin cancer is grouped as Non-Melanoma skin cancers [4].

Melanoma skin cancer is due to abnormal growth of pigmented skin cells called Melanocytes. Upper most layer of skin contains melanocytes. Melanocytes are those cells that gives skin its color.

Skin cancer has ability to spread from primary region to the secondary region called Metastasis. It grows rapidly if not detected or treated timely. Ultraviolet rays' damages DNA and causes irregular growth of skin cells.

Melanoma is fatal type of skin cancer. Melanoma have highest mortality rate among all type of skin cancers so it's very important to diagnose cancer at early stages. Early diagnosis is crucial for reducing mortality rate. Melanomas have different shapes and sizes. It also varies in its color. Since it's a very hard challenge to determine melanoma. If detected early, survival rate increases up to 98% [5].

Early Diagnosis of skin cancer can increase the chance of managing the disease in a better way. According to research experts, early detection lead to survival to patient. As we know, melanoma is aggressive in nature due to metastasis. The growing rate of melanoma is faster the other skin cancers. Globally, researchers are trying to innovate methods, so melanoma could be controlled. Following are the problem which are addressed by this thesis.

- Prevalence rate of skin cancer is on the higher side and especially that of melanoma

- Melanoma is aggressive in nature due to its high metastasis rate; therefore, timely diagnosis is critical for its treatment before the onset of malignancy.
- Various methods have been employed ranging from visual inspection to the textural analysis of the Dermoscopic images.
- However, accuracy of these methods is still undesirable for proper clinical treatment because of the sensitivity involved in surgical or drug application.
- Against this backdrop, this emphasizes on the development of an automated model with promising accuracy so it may be used in a clinical setting.

Statement of Purpose

The existence of the IEEE International Symposium on Biomedical Imaging (ISBI) 2017 Challenge [6] for Skin Lesion Analysis Towards Melanoma Detection has provided this project with a useful dataset, the ISIC Archive dataset [7], which contains dermoscopic images paired with their corresponding lesion binary masks, and the possibility of benchmark the results obtained against other participants.

The organization of the challenge provided the possibility of benchmark the results obtained against the top-ranked participants and evaluate how well our model performs. Moreover, the organization provides a guideline of how to develop the entire project by dividing the work into three parts: (I) Lesion Segmentation, (II) Lesion Dermoscopic Feature Extraction, (III) Lesion Classification [28], in particular, the organization proposed a subsection involving a previous segmentation of the lesion in order to study if this technique improves or not the segmentation task. This project has followed the specifications and evaluation metrics proposed by the ISIC 2017 Challenge.

Statistics of Melanoma

Melanoma are most common type of cancer. Early treatment is very crucial for proper treatment. Frequency of melanoma is outpacing all types of cancer over the past three decades.

In United States, skin cancer is among one of the most common cancer in young men and women. Some statistics of melanoma are:

- Almost one person dies of skin cancer every hour.
- Risk of developing melanoma is 2.5% in whites 0.1% in blacks over life span [8].
- Approximately, 1 million diagnosed cases of melanoma worldwide in 2018 [9].
- Around 96,000 cases of melanoma are expected to diagnose in 2019 [10].
- Average age of patients diagnosed with melanoma is 63 years [11].

Objectives

The main objective of the thesis is to develop an automated algorithm to detect region of interest (ROI) for a better diagnosis of cancer patients. Accurate region extraction is very important for better diagnosis. Following are objectives to achieve this goal:

- 1) Developing methods for an objective and time-efficient tool for diagnosing skin lesions based on digitized dermoscopic color images
- 2) Increasing diagnostic accuracy for proper treatment
- 3) Early detection of melanoma that significantly increases survival rate.

This study is categorized into the following objectives to achieve the goal of research.

Designing of Algorithm

Deep Learning Algorithm is designed for segmenting skin lesion. This section involves data acquisition, training of deep learning model, and pre-processing on dataset. This section further involves the optimization of the designed algorithm.

Model Testing

Algorithm is evaluated on a test group to check whether algorithm is segmenting accurately and comparing results with the existing techniques and other participants of the challenge based on evaluation metric

CHAPTER 2

Literature Review

CHAPTER 2: Literature Review

Deep learning architectures have been used for object detection, image recognition and pattern recognition. They are used as fully automated methods for different tasks i.e. Image Classification and Image Segmentation. Most of the methods were relying on state-of-the-art hand-engineered low-level descriptors. But since the arrival of artificial intelligence, most of the techniques were relying on learning image features using Deep learning architectures.

Literature depicts existing state of the art methods that are used for segmenting image or extracting Region of Interest (ROI). i.e. Region-Based techniques, Edge Detector, Thresholding Techniques, k means clustering, Fussy c means. et cetera. Feature Extraction is based on some machine learning algorithms such as Artificial Neural Network (ANN), k-nearest neighbor (KNN).

Imaging Techniques

There are different methods of acquiring dermoscopic images. There are some non-invasive methods usually used for assisting researchers and dermatologists for examining skin lesions. Some of them are:

- Photography
- Dermoscopy
- Confocal Scanning Laser Microscopy (CSLM)
- Optical Coherence Tomography (OCT)
- Ultrasound Magnetic Resonance Imaging (MRI)
- Spectroscopic Imaging

Table 1. Imaging Techniques

Imaging Technique	References
Spectroscopic Imaging	[12] [13]
Macroscopic Images	[14] [15] [16]
Epiluminescence Microscopy (ELM)	[17] [18] [19]

Table 1 explains some common imaging techniques used to acquire dermoscopic images. ELM acquired images are also known as “Dermatoscopy Images”. Macroscopic images are also known as “Clinical Images”. Skin images are obtained by using digital cameras. According to literature, conditions under which images captured are not definite. Following factors may change.

- Variable Illumination conditions
- Variable distance from lesions
- Poor resolution

These factors may cause complications while examining skin lesions, especially when lesion size is small. There are other various issues regarding skin images i.e. Hair artifacts, shadows, reflection and lines present on the skin.

Epiluminescence Microscopy (ELM)

Epiluminescence microscopy is a non-invasive technique to capture skin lesion images. ELM is most commonly used technique for acquiring skin images. It consists of a light source and magnifying glass. Lesions are immersed in oil before examining. Most importantly, this technique aids in differentiating between the malignant tumor or benign. Researchers and dermatologist use this technique for expert opinion because some lesions are not properly visible with the naked eye so, dermatoscopy increases the accuracy of examination up to 20% [20]. Figure 1. shows a dermatoscope.



Figure 1. Dermatoscope

Some associated work based on manual feature extraction are:

- Quoc-Bao et al. [21] elaborates techniques based on local binary patterns (LBP), color histogram and edge histograms.
- M.Ruela et al. [22] suggested that color features are more significant than texture features. They propose two methods for detecting melanoma through dermoscopic images.

Pre-Processing Techniques

Preprocessing is considered as an important preliminary step while segmenting image. Researchers has faced difficulties while segmenting images due to low contrast of the images. Some of the images has some artifacts that has to be removed for better segmenting and getting good results. Literatures shows some preprocessing methods that are commonly used in machine learning before feeding data to architecture. Celebi et al. [23] devised a technique that increases contrast of the image by determine ideal weights for converting RGB image to Gray scale image by maximizing Otsu's histogram bimodality measure. Rajab et al. [24] proposed a theory that the size of filter that is being applied on the image must be proportional to the size of the image for better smoothing of image. Proposed technique has significant segmentation results. Lee et al. [25] proposes a preprocessing tool to remove hair like structures from the

dermoscopic images using morphological operations. Salt and pepper noise have bad effects on the segmentation. A median filter is operative on eradicating noise from images [26].

Table 2. State of the art pre-processing methods

Preprocessing Methods	References
Color Space Transformation	[27] [28]
Illumination Correction	[14] [29]
Contrast Enhancement	[27] [28] [30]
Artifact Removal	[27] [25]
Removing Shadow Effect	[31] [24]

Table 2. explains renowned pre-processing method commonly used in literature. Hassan et al. [32] introduced a pre-processing technique that converts that RGB images to CIE l^*a^*b color spaces. These color space has a controlling effect on the contrast of the images. They augment the assessed perceptual regularity of image colors. Glaister el al. proposed a method that correct illumination variations in macroscopic images.

Image Segmentation

Image segmentation is a process to extract the region of interest from the given image. Process is continued until ROI is detached from image background. There are some noticeable issues that may cause issues while segmenting skin lesions such as skin lines, bubbles, shadows and hair structures. To remove these artifacts, previously defined pre-processing methods are used to increase the performance of algorithm. There are various techniques used to segment images. i.e. edge based, thresholding-based methods, clustering methods, adaptive stochastic methods et cetera. Table 3. summarizes the existing state of the art segmentation methods.

Table 3. Segmentation Methods

Segmentation method	Technique	Reference
Edge based Thresholding Based	Edge Detector	[33] [34]
	Otsu's Thresholding	[17] [22]
	Fuzzy Logic	[18]
	Adaptive Thresholding	[27] [33] [31]
Region-based	Region Growing	[32] [35]
	Statistical Region Merging	[29] [23]
AI Based	Neural Networks	[36] [37] [38][39]
	Fuzzy Logic	[17]
Active Contour Based	K-means Clustering	[40] [41] [42]
	Adaptive snake	[17]
	Level Set	[43]
	Expectation -maximization level set	[17]
Other Methods	Hill Climbing Algorithm	[27]
	Dynamic Programming	[44] [45]

Artificial Intelligence Based Methods

This thesis is focused on AI based methods for segmentation purpose. In neural networks, the pixels of images are classified to detect the region of interest from the input images. Fuzzy c-means, k-means and neural networks are examples of those techniques which are like humans in sense of learning and natural conditioning. Additionally, these techniques are combined with the pre-processing techniques to increase the segmentation results.

AI based algorithms are applied to segment the skin lesion images and achieved promising results.[36]. Genetic algorithms (GA) are also combined with AI to increase the performance of models.[46] Genetic algorithms are based on natural evolution to find a solution for a practical application just like humans. Robert et al. proposed a method that segments skin lesion through genetic programming. This technique is based on natural evolution and creates random population from sets. Terminal set is the designed from the embedded information in the input images i.e. shapes and textures of the images.[47]

Fuzzy logic algorithms are also used to segment skin lesions.[48][49]. Fuzzy logic deals with imprecise values. Fuzzy logic is applied with merging it with other methods. Data is analyzed quantitatively in fuzzy mean. Maeda[48] introduced a method that combines the textural information and color features of the images to segment skin lesions.

Active Contour Based Segmentation

Clustering based methods are also used for segmenting skin lesion images. Temiselvi et al. [50] proposes a method based on k-means clustering. Castillejos et al. proposed a method that takes insights from a combination of methods i.e. k-means , FCM and CPSFCM algorithms. [48] introduced a method “HCA” that takes input image as one parameter and histogram bins of every dimension as other parameter. The output of proposed algorithm is a labeled image. In traditional k-means method, clusters are formed on manual interpretation by user.

Level set and region growing methods have some limitations. Abbas et al.[45] proposed a technique which have good edge detection capabilities. This algorithm is computationally well-organized and effectively look for local minima and overlapping issues. Literature depict that different clustering-based methods are combined to increase the performance of algorithm by accurate segmentation of skin lesion images.

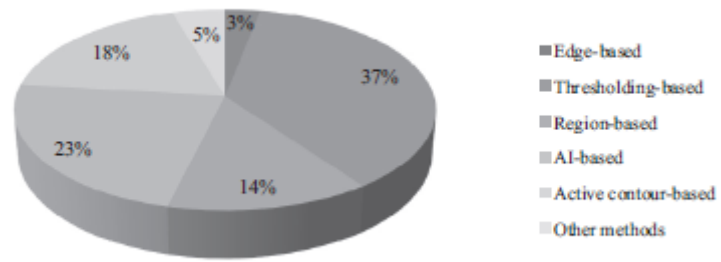


Figure 2. Distribution of methods according to applied principle

Methodology

CHAPTER 3: Methodology

Methodology

This thesis advances a study in Deep learning field about the influence and adjustments of removing skin image background by applying a semantic segmentation according to classification of disease. By comparing results, this work aims to perform better while segmenting skin images. This article explains the binary segmentation of skin images to extract ROI from Dermoscopic images.

To achieve our goal, a well know CNN architecture for segmentation has been adopted.

Dataset

The ISIC 2017 challenge dataset for Skin Lesion Analysis towards Melanoma Detection was used in this work. The dataset is publicly available and contain 2750 RGB images that are pre-partitioned into 2000 training images, 150 validation images and 600 test images. All images include binary masks to label the lesion within the image. For further evaluation, we have used another public dataset named as PH² dataset. It consists of 200 dermoscopic images.

Table 4. ISIC Dataset Distribution

Groups	Total Images
Training Set	2000
Validation Set	150
Test Set	600

Pre-Processing

Images in the dataset vary in their sizes. They is a need to apply some preprocessing techniques on the dataset. In CNN, image is preprocessed before giving as an input to the network to avoid complexities and computational time. Time is a major concern while training a network, so

images are preprocessed to reduce training time and computational cost required to train a network. Following are the preprocessing steps performed on the Dataset.

- Image Scaling
- Hair Removal
- Image Standardization and Normalization
- Rotation
- Median Filter

Image Scaling

Training images contain 2000 dermoscopic images. All images are RGB and in '.jpg' file format. All images vary in the sizes. Image are reshaped to 256×256 resolution to make ease for neural network to convolve faster with taking less time for computing results. It saves computational cost and time.

One thing must be noticed while reshape the image to the smaller dimension that too small dimension causes the pixel distortion and missing out many important information from the image. Anti-Aliasing filter clear out this noise or distortion while reducing image dimension and a suitable dimension of 256×256 is chosen so that image embedded information must not loss.

Hair Removal

Most of the images are present with the hairs on image that act as a noise while segmenting lesion. So, it's important to remove these artifacts before giving images to neural network. Neural network act better on the images without hairs. Hair removal algorithm is divided into 3 steps that are required to remove hair like distractions from the image.

- Conversion of RGB into Grayscale Image

- BlackHat filter is applied on the grayscale image and image contain hair structures is obtained.
- Obtained image is thresholded at a certain point to obtain a binary mask
- Binary mask and the original image is inpainted to replace the hair structures with the neighboring

RGB image is converted to grayscale image to take only one channel to implement morphological operations on the image. This is done with a python library “OpenCv” that converts the RGB image to grayscale.

Image Inpainting

Image inpainting is a technique to restore distorted images and used to remove noise from the image. Unwanted part is removed from the image and those regions are inpainted with the pixel values in the neighboring of that region. Image inpainting based on Fast Marching Method. Image inpainting method is used as function “cv2.inpaint” from python library named as “OpenCv”.

Inpainting requires two variables as an input. One is the original image on which we want to inpaint and the other is a binary mask, that defines the pixel location we want to inpaint. For inpainting a point p , algorithm takes a small neighborhood ε . The value of the p comes from the known region. First iteration is defined as:

$$I_q(\mathbf{p}) = I(\mathbf{q}) + \nabla I_q(\mathbf{p} - \mathbf{q}) \quad \text{—Equation (1)}$$

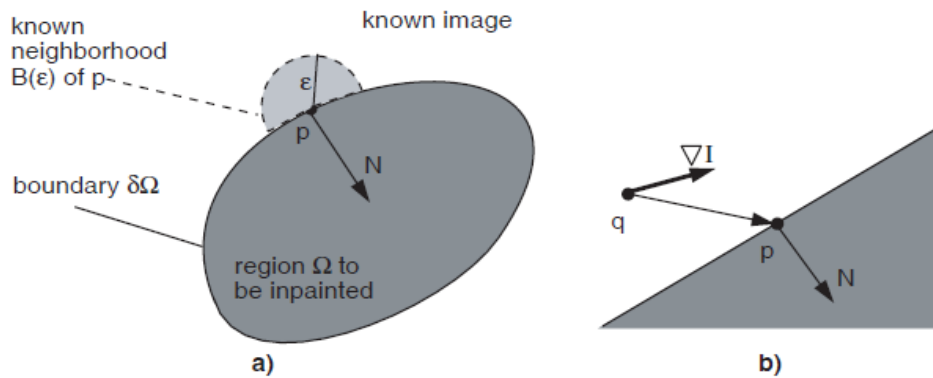


Figure 3. Image Inpainting pixel plane

Image Standardization and Normalization

Image Standardization is the method to rescale data so that it has 0 mean and 1 standard deviation. Image normalization is processing technique that scale image pixel values from 0-255 to 0-1. It is the most common technique used in the CNN to save computational power. Neural network process inputs by multiplying the inputs with a small weight and then takes gradients of the inputs. So, it's a good practice to normalize the image so that values are reduces so that gradient will not explode while going in deeper layers. Image Normalization is used to zero centered the data. All image features are on same scale. Zero centering is done by subtracting the mean of image from the image and then dividing by the standard deviation. Image normalization is defined by an equation.

$$\mathbf{Image\ Normalization} = \frac{\mathbf{Image - mean\ of\ Image}}{\mathbf{Standard\ Deviation\ of\ Image}} \quad \text{--Equation (2)}$$

Mean is subtracted from all channels of the image. Normalization also resembles the contrast stretching and it is used as a common practice because there are image in the dataset with poor contrast. Dataset resembles the normal distribution. Figure 8. shows the distribution of the images after normalization of images.

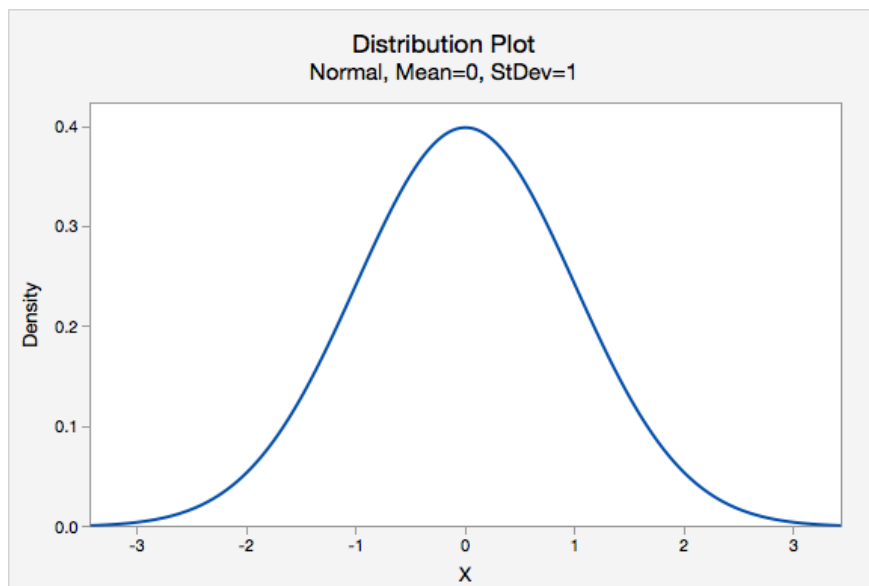


Figure 4. Image Data Distribution

Rotation

One of the biggest drawbacks of neural network is large requirement of dataset. For a good training, dataset is augmented by rotation of the images, along with their respective ground truths. Neural network takes large data to generalize and perform better. So, augmentation is done to increase the dataset, to increase the performance of the model. By augmentation techniques, new images are introduced to model so model can predict accurately.

Median Filtering

After removing hair artifacts, there is still a noisy part in the image which is removed by applying median filtering. Median filtering not only blur the image but remove a significant portion of noise from the image. Median filter is operative in removing “pepper and salt” noise from the image. A kernel is specified for applying median filter.

Network Architecture

Encoder Decoder based Architectures

The encoder decoder-based architecture is employed in this research. The encoder is the network that takes input image and extracts feature maps from the image. In encoder, down sampling occurs, and image is down sampled to smaller dimension to extract features from the image. Layers closer to the input extracts features i.e. edges, pattern , lines, texture , while those layers which are close to the output determines the shape and close of the image. In this way information is extracted from the image. The features which are extracted represent the input image given to the encoder. The encoding path is also known as the contracting path because image dimension are decreased. There are different encoder architectures i.e. ResNet, Inception , VGG16, ResNext et cetera.

Decoder takes the feature maps from the input and maps the input features to the actual input size or intended input size. Decoder is a simple architecture that receives the input in the form of feature maps and then up sample image dimensions until original input size is obtained. In decoder, deconvolution happens. Upsampling is done by increasing dimension and merges it with the layer coming from encoder of same dimension to map the features to the accurate pixel values in the original image. The most popular decoder architecture used in Deep learning applications is U-NET.

ResNet 50

Encoder employed in our research is ResNet architecture. ResNet has a unique advantage over other encoders. As we know, in deeper network there is a problem of gradient vanishing. In ResNet, there is feed forward loop that flows in forward direction by two ways. One is the main path and the other is the identity block. The vanishing gradient issue is addressed by the ResNet Architecture.

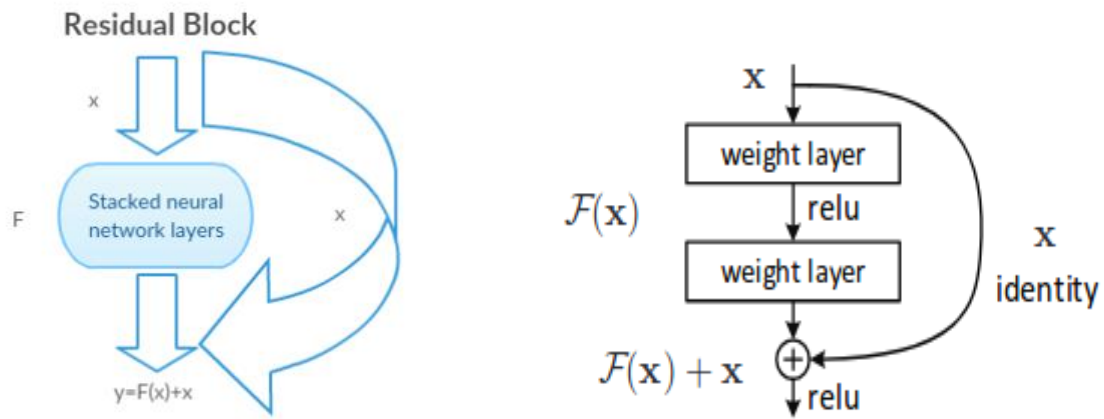


Figure 5. Residual Block of ResNet 50

An RGB input is given to the model and a 3×3 filter is applied to a 3-channel image.

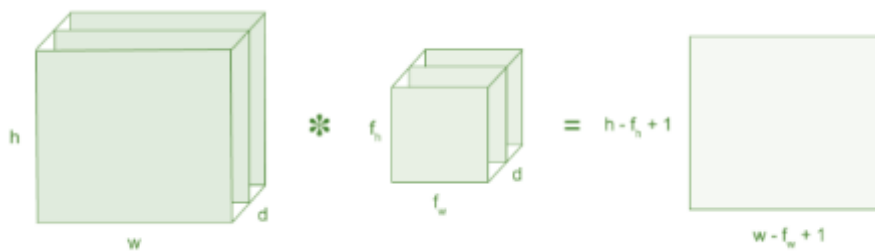


Figure 6. 3-Channel Convolution

U-Net

On deconvolutional side, we have used U-Net architecture. In decoder, upsampling occurs that increases the image dimension by simply zero-padding input dimensions and increases the output size. Decoder takes the features map that are extracted by the encoder and maps those features on the pixel wise location in the upsampled image. Basically, decoder works by merging two layers. One that is coming from the encoder to the one that upsampled in the decoder. In short, feature maps are very pixel-wise sensitive so, merging those arrays maps those features in the image. The upsampling occurs until the original dimensions are obtained.

The output of the decoder is 256×256 equal to out input dimension. Last layer used in our decoder architecture is a Sigmoid layer. In semantic segmentation, our goal is to classify the image pixel with the classification. In a binary classification, we have two classes i.e. 0 or 1. The array received at the end of the Decoder is a pixel-wise probability of the image.

In decoder, a term named as “Transpose Convolution” is used. It is the reverse of the convolution. It upsamples the dimensions with a learnable parameter. It is done because after extracting features, we need to define where to put the information because at the end we need a pixel-wise representation where, each pixel explains the class of that pixel.

Sigmoid Layer

A sigmoid layer is deployed at the end of architecture in semantic image segmentation that applies sigmoid function on the pixels and gives the probabilities of that pixel. A sigmoid function is explained by an equation.

$$\text{Sigmoid} = \sigma(z) = \frac{1}{1+e^{-z}} \quad \text{—Equation (3)}$$

Sigmoid maps pixel probabilities between 0 or 1. An X-axis shows the pixel intensities and y-axis scale these pixels intensities between 0 or 1.

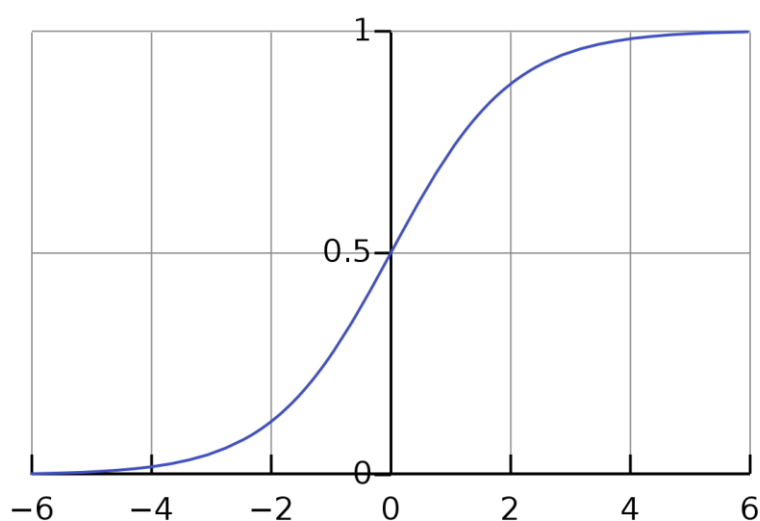


Figure 7. Sigmoid Function Graph

Hyperparameters

Hyperparameter are those parameters that are given before the training process. These parameters are different for different architectures. Model can learn by the adjustment of these parameters. Optimization of these parameter largely affect the training process and help network learning best features. Some of the important parameters are epochs, batch size, optimizers et cetera.

Optimizers

Deep learning is highly dependent on the iterations while training and training is heavily dependent on the hyperparameters. Selection of hyperparameters is very important to optimize the cost function. The cost function is explained as;

$$J(W, b) = \sum_{i=1}^m L1(y', y^i) \quad - \text{Equation(4)}$$

The purpose of the optimizer is to optimize this cost function. J is the mean value obtained by the loss function between the actual label and the predicted label given to the network. On the basis of loss, model updates the value of weights and the bias. W is the weights and b is the bias in above mentioned equation.

Gradient Descent

A gradient descent is a iterative function used to find the local minima. At the start of the training, a weight matrix w is initialized randomly. The gradient descent is used to find further optimal weights and to minimize the cost function. Following equations are used to explain the gradient descent in deep learning cases.

$$W = W - \alpha \frac{\partial}{\partial W} J(W) \quad - \text{Equation(5)}$$

$$b = b - \alpha \frac{\partial}{\partial b} J(b) \quad - \text{Equation(6)}$$

Considering Equation 5, two possible cases are:

- 1) If weights values are initialized less than that required for the minima , partial derivative is negative according to Equation 5. Hence weight values are increased.
- 2) If weights values are initialized greater than required for the minima , partial derivative is positive. Hence weight values are decreased

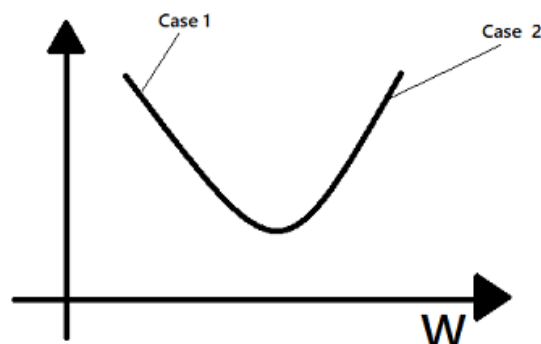


Figure 8. Gradient Descent

Figure 8 explains the case 1 and case 2, when weights are initialized randomly. The disadvantages of the gradient descent is that it updates the weights and bias once it go through all data so, in those case where data is very large and it doesn't fit into the computer's memory, complications arises.

Adam Optimizer

In order to address our problem of optimization, we have used Adam optimizer due to its following advantages.

- Reduces training time of the model
- Network converges faster.
- Reduces overfitting.
- Computationally efficient.
- Well suited to Deep Networks that are large in terms of parameters.

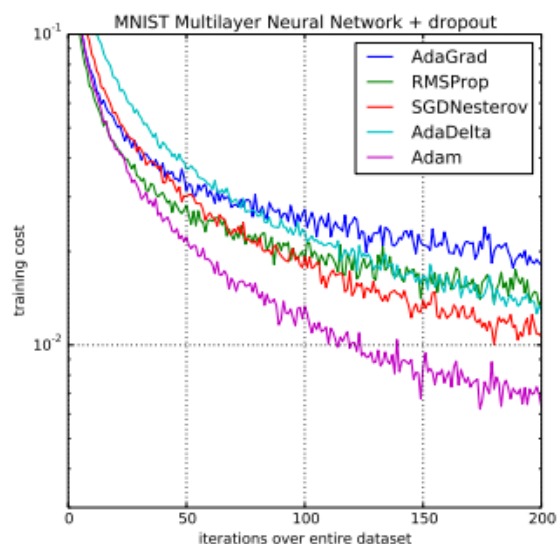


Figure 9. Comparison of Adam with other optimizers

In deep networks like ResNet, Adam is the only choice because there are a million of learnable parameters. Adam optimizer can efficiently optimize cost function where data is large. Kingma et al. [52] proposes Adam and compares Adam with other available optimization methods on MNIST Digit Recognition Challenge [53].

Loss Function

Binary Cross-entropy

Binary cross entropy is a measure to evaluate the performance of the network. It is also defined as the log loss. Loss increases as the predicted label diverges from the actual label. On x-axis , there is a probability of the predicted label and on y-axis negative log of probabilities is plotted. When the probability goes closer to 1, log loss decreases in exponential manner. Binary cross-entropy is applied when the output is always between two classes i.e. 0 or 1.

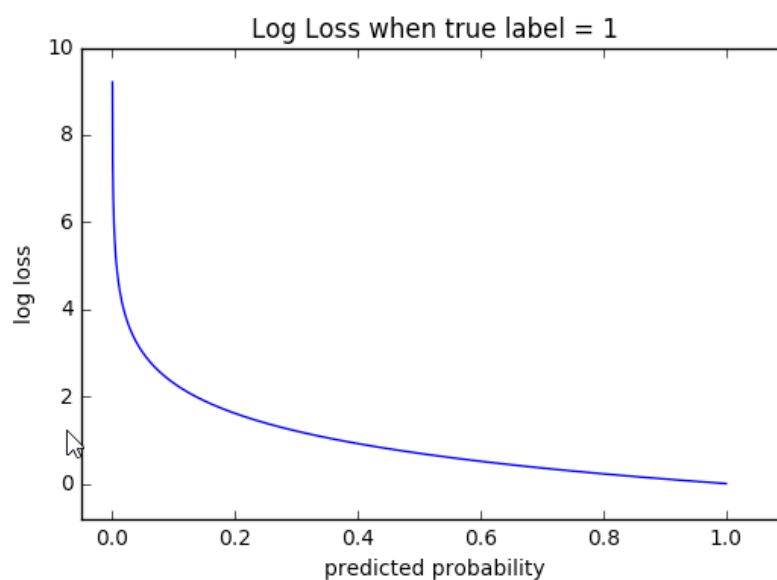


Figure 10. Log Loss

Evaluation Metrics

The similarity between actual label and the predicted label is determined by the evaluation metrics. Following Metrics are used for evaluating our network.

Accuracy, which computes the number of correct predictions divided by the total number of samples.

$$\text{Accuracy} = \frac{\text{Number of Correct Prediction}}{\text{No of Samples}} \quad - \text{Equation(7)}$$

Dice coefficient is computed by comparing the pixel-wise agreement between the ground truth (Y) and its corresponding predicted segmentation (X). Specially, this metric is just used to evaluation the segmentation model performance.

$$\text{Dice Score} = \frac{2TP}{(TP+FN)+(TP+FN)} \quad - \text{Equation(8)}$$

Jaccard index, also known as the Jaccard similarity coefficient, compares predictions (A) with the ground truth (B) to see which samples are shared and which are distinct. The higher the index, the more similar the two subsets.

$$\text{Jaccard Index} = \frac{TP}{TP+FP+FN} \quad - \text{Equation(9)}$$

Sensitivity, also known as recall, is computed as the fraction of true positives that are correctly identified.

$$\text{Sensitivity} = \frac{\text{Number of True Positives}}{\text{Number of True Positive+Number of False Negatives}} \quad - \text{Equation(10)}$$

Precision, which is computed as the fraction of retrieved instances that are relevant.

$$\text{Precision} = \frac{\text{Number of True Positives}}{\text{Number of True Positive+Number of False Negatives}} \quad - \text{Equation(11)}$$

Specificity computed as the fraction of true negatives that are correctly identified.

$$\text{Specificity} = \frac{\text{Number of True Negative}}{\text{Number of True Negative} + \text{Number of False Positive}} \quad - \text{Equation(12)}$$

The important metrics for evaluation are:

- 1) Jaccard Index
- 2) Dice Score

Jaccard Index:

Jaccard Index is a very important metric to find a similarity between two sets A and B. A is a matrix of predicted label and B is a matrix of actual label.

$$\text{Jaccard Index} = js(A, B) = \frac{|A \cap B|}{|A \cup B|} \quad - \text{Equation(13)}$$

Jaccard Index is defined as the ratio of intersection of two sets by union of two sets. The more the value of Jaccard Index, more similar the population of two sets. Jaccard Index is a pixel-wise similarity of the two sets. One of the disadvantages of the Jaccard index is small size of sample set. Jaccard Index gives erroneous results when sample size is small.

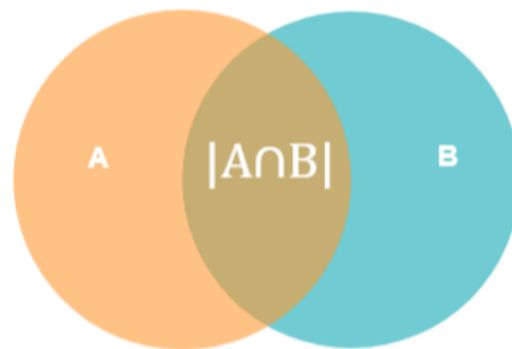


Figure 11. Jaccard Index Overlap

Figure 11 explains the partial overlap of set A and B which is represented by $|A \cap B|$.

Dice Coefficient

Dice coefficient is measuring coefficient to determine the similarity between two samples. Dice score checks the spatial distance between pixels to determine similarity between two sets. Dice can also be applied on discrete data.

$$\text{Dice Score} = \frac{2TP}{(TP + FN) + (TP + FN)} \quad - \text{Equation(14)}$$

Dice coefficient can be differentiated from Jaccard index in the sense of confusion matrix that Jaccard count true positives once in denominator and numerator.

- 1) Dice coefficient is 1 , if there is complete overlap of set A and B.
- 2) Dice coefficient is from $0 < DSC < 1$, if there is partial overlap.
- 3) Dice coefficient is 0, if there is no overlap.

Results

CHAPTER 4: Results

Skin Lesion Segmentation

We trained our model named “ResUNet” on the ISIC 2017 dataset. This performed the automatic prediction of the skin lesion from the Dermoscopic images taking the form of binary masks.

An example representation of input images to be classified, with ground truth and predicted label is shown in Figure 12 (a).

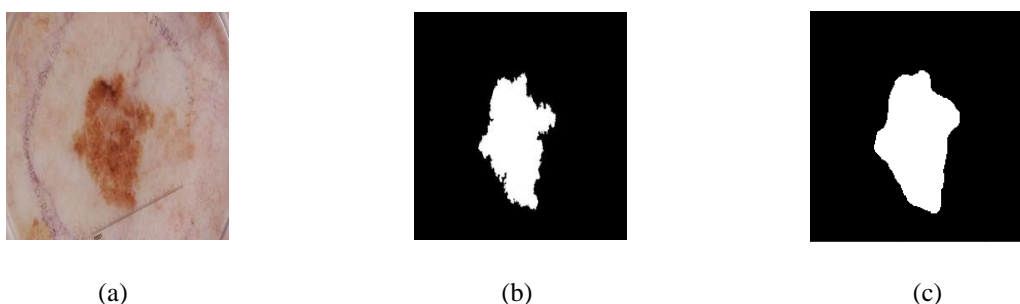


Figure 12. Example Images: (a) Original image, (b) Original binary mask, (c) Automated predicted mask

Pre-Processing

Hair Removal Algorithm

As most of the images contain hair artifacts that interfere with proper segmentation of the lesions, the hair removal algorithm is applied. The RGB images are converted to grayscale and then passed onto the blackhat filter.

BlackHat Filter

Black Hat filtering is obtained by subtracting closing of image from original image. If A is original input image and B is closing of input image, then Black hat filter is defined by an equation:

$$\mathbf{Black\ Hat(A) = Abh = (A \cdot B) - A} \quad \text{-- Equation (15)}$$

Image closing is morphological operation that is defined as the erosion of the dilation of set A and B. A is defined as the image and the B is defined as the structuring element. Hair structures are straight lined structures so, best chosen structuring element is cross shaped structuring element having pixel values in lines.

```
[0 0 0 0 0 0 0 0 1 0 0 0 0 0 0 0 0]
[0 0 0 0 0 0 0 0 1 0 0 0 0 0 0 0 0]
[0 0 0 0 0 0 0 0 1 0 0 0 0 0 0 0 0]
[0 0 0 0 0 0 0 0 1 0 0 0 0 0 0 0 0]
[0 0 0 0 0 0 0 0 1 0 0 0 0 0 0 0 0]
[0 0 0 0 0 0 0 0 1 0 0 0 0 0 0 0 0]
[0 0 0 0 0 0 0 0 1 0 0 0 0 0 0 0 0]
[0 0 0 0 0 0 0 0 1 0 0 0 0 0 0 0 0]
[1 1 1 1 1 1 1 1 1 1 1 1 1 1 1 1 1]
[1 1 1 1 1 1 1 1 1 1 1 1 1 1 1 1 1]
[0 0 0 0 0 0 0 0 1 0 0 0 0 0 0 0 0]
[0 0 0 0 0 0 0 0 1 0 0 0 0 0 0 0 0]
[0 0 0 0 0 0 0 0 1 0 0 0 0 0 0 0 0]
[0 0 0 0 0 0 0 0 1 0 0 0 0 0 0 0 0]
[0 0 0 0 0 0 0 0 1 0 0 0 0 0 0 0 0]
[0 0 0 0 0 0 0 0 1 0 0 0 0 0 0 0 0]
[0 0 0 0 0 0 0 0 1 0 0 0 0 0 0 0 0]
[0 0 0 0 0 0 0 0 1 0 0 0 0 0 0 0 0]
```

Figure 13. 17×17 Cross shaped Structuring Element

A 17×17 cross shaped structuring element is used. While applying closing morphological operation, dilation grows the structures in the image pixel representing with the structuring element whereas, erosion removes the small boundary pixel that are representing the structuring element. Image obtained after applying closing is the image without hair like structures. To obtain the hair like structures, this resulting image is subtracted from the grayscale image.

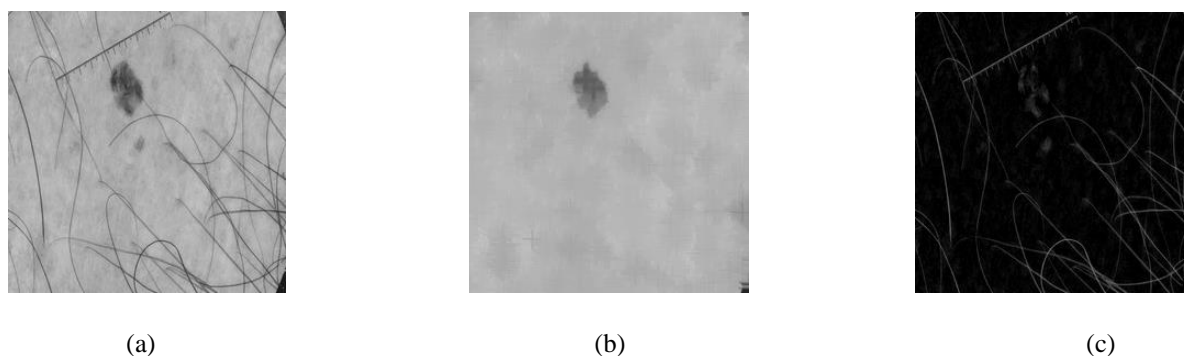


Figure 14. Representation of a single image as it is passed through the Hair Removal Algorithm. Left to right: (a) Grayscale image. (b). Image obtained after closing. (c) Image obtained after applying Black hat Filter.

Figure 14 (c). represents the image obtained after applying the BlackHat filter. Hair like structures are obtained. For applying Image inpainting we, need a mask that defines the pixel location where we want to inpaint the image and the original image in which we want to inpaint. For this purpose, threshold of 10 is defined. It means those pixel values which lies in the range of 0 to 10 are extracted as binary image mask. 0 represent the black pixel and 1 represents the white pixel. Thresholding is applied by a function in python library “OpenCV”.

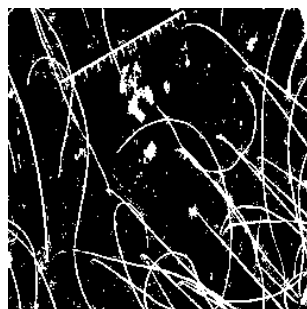


Figure 15. Thresholded Binary Mask

The inpainting algorithm replaces the hair structures with the bordering pixels of the image to restore the original image. This technique is commonly used in recovering old or noisy images. Image to be inpainted and the mask obtained after thresholding (figure 15) is used to inpaint

those hairy regions that are extracted with the neighboring pixels and output is achieved (figure 16).

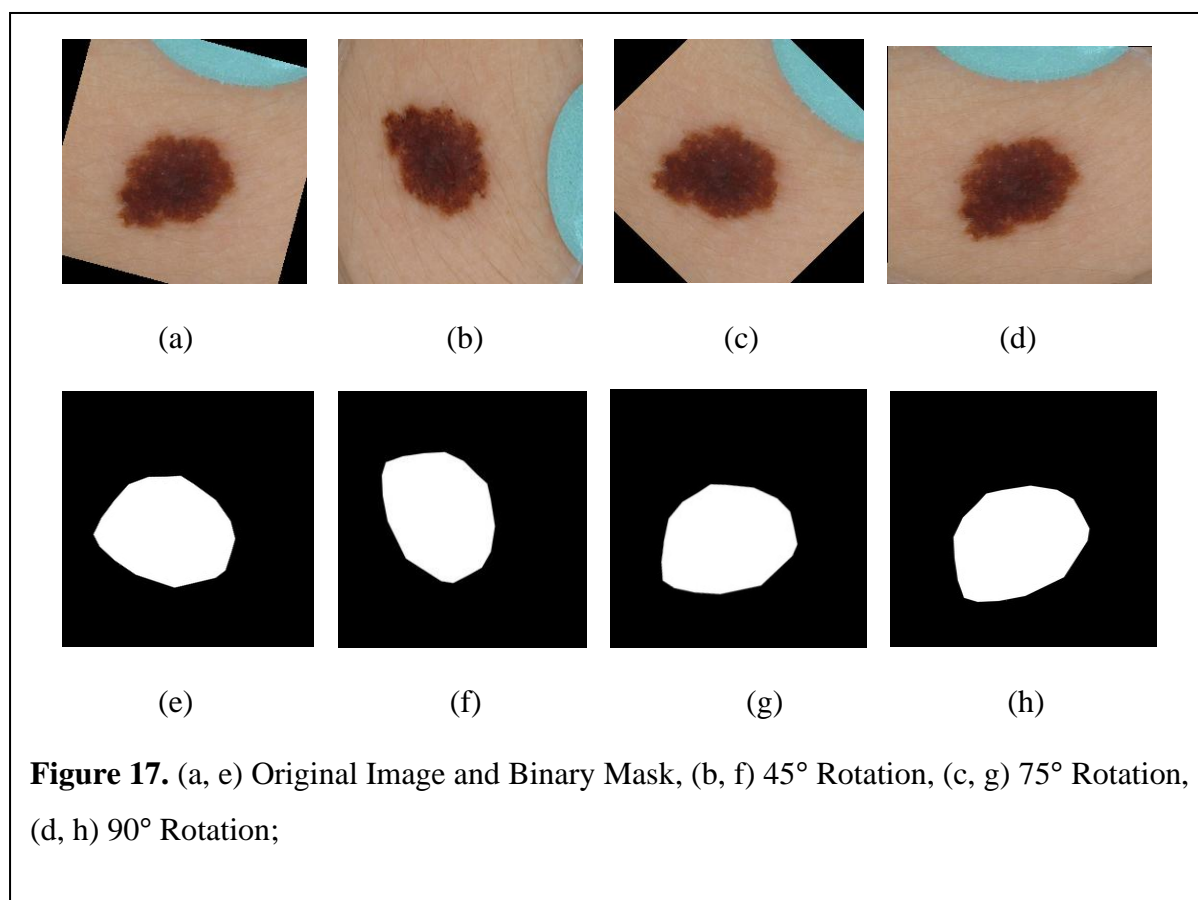


Figure 16. Final inpainted image.

Rotation

Training images, as provided by the ISIC, are composed of 2000 images. One of the biggest drawbacks of neural network is the requirement of large datasets. For a good training of the model, dataset is augmented by rotation of the images. Image augmentation is done at 3 angles to increase three times training dataset. After applying image augmentation, we have 8000 training images. The rotation of images is done at following angles, and examples results of the images along with their labels are shown in Figure 17.

- 45° Rotation
- 75° Rotation
- 90° Rotation



Images are rotated along with their respective ground truths. Neural network takes large data to generalize and perform better. So, augmentation is done to increase the dataset, to increase the performance of the model. By augmentation techniques, new images are introduced to model so model can predict accurately.

Network Architecture

A basic block diagram, representing the general steps employed during the process of the work, is demonstrated in Figure 18.

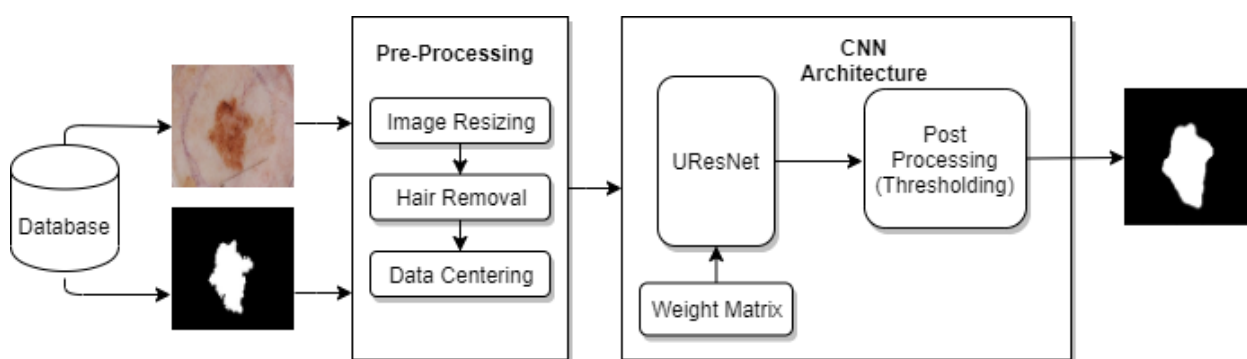


Figure 18. Training Block Diagram

ResNet 50

Encoder employed in our research is ResNet architecture. The contracting path is composed of input layer and a series of Convolutional, Max-pooling and Batch Normalization layers. In convolutional side, an input of 256×256 is given. Max pooling layer is defined after the first convolutional layer with a stride of 2 that halves the dimension of the image. A kernel of 3×3 is defined that applies a max function and divides the dimensions into half. A series of repetitive blocks are defined, that involves convolutional layer followed by a batch normalization layer, Relu-Activation layer. In ResNet 50, the numerical number denotes the depth of a network. In deeper ResNet, a bottleneck block is introduced, that decreases the channels of the image by 1×1 convolution before dominating 3×3 convolutional layer. The purpose of the bottle neck architecture is to save computational time, required for training the architecture. After 3×3 convolutional layer, again 1×1 convolutional layer is defined to restore the dimension of the image. An RGB input is given to the model and a 3×3 filter is applied to a 3-channel image.

Image Dimensions are given as $(h \times w \times d) = (256 \times 256 \times 3)$

Filter Dimensions are given as $(f_h \times f_w \times d) = (3 \times 3 \times 3)$

Output is $(h - f_h + 1) \times (w - f_w + 1) \times$

Mathematical implementation shows, RGB image when convolves with the 3 dimensions 3×3 filter, output is a single dimension feature map.

The encoding path architecture is explained in the table given below.

Table 5. Encoder Architecture

<i>Layer Name</i>	<i>Output Size</i>	<i>Kernel Size & No of filters</i>
Max Pooling	128×128	3×3 , Stride 2
Conv 1	64×64	7×7 , 64, Stride 2
Conv 2	64×64	$\begin{bmatrix} 1 \times 1 \times 64 \\ 3 \times 3 \times 64 \\ 1 \times 1 \times 256 \end{bmatrix} \times 3$
Conv 3	32×32	$\begin{bmatrix} 1 \times 1 \times 128 \\ 3 \times 3 \times 128 \\ 1 \times 1 \times 512 \end{bmatrix} \times 4$
Conv 4	16×16	$\begin{bmatrix} 1 \times 1 \times 256 \\ 3 \times 3 \times 256 \\ 1 \times 1 \times 1024 \end{bmatrix} \times 6$
Conv 5	8×8	$\begin{bmatrix} 1 \times 1 \times 512 \\ 3 \times 3 \times 512 \\ 1 \times 1 \times 2048 \end{bmatrix} \times 3$

A 3×3 convolutional layer in each down samples the image dimensions. An input is given of 256×256 and after Conv5 it reduces to 8×8 dimension with 2048 number of filters.

U-Net

On deconvolutional side, we have used U-Net architecture. In a binary classification, we have two classes i.e. 0 or 1. The array received at the end of the Decoder is a pixel-wise probability of the image. The output of the decoder is 256×256 equal to input dimension.

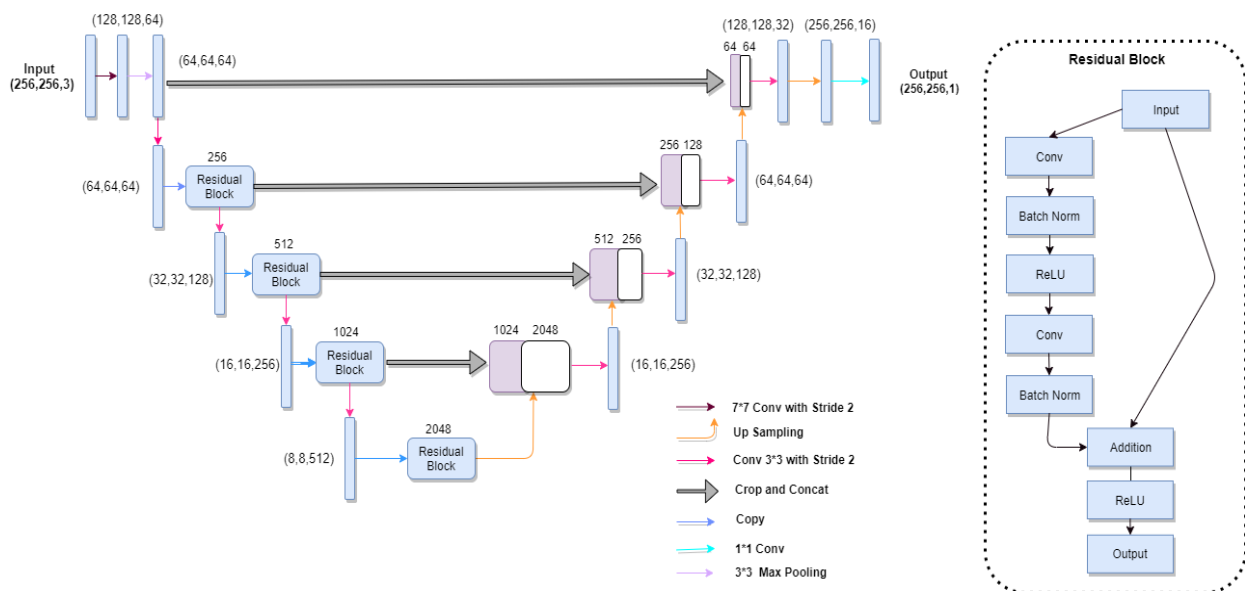


Figure 19. Schematic diagram representing UResNet-50. The encoder shown on the left is the ResNet 50, while the U-Net decoder is shown on the right. Given in the parenthesis is the channel dimensions of incoming feature maps to each block. Arrows are defined in the legend.

The network architecture (as shown in Figure 19) takes insight from both U-Net and ResNet. The contracting path (convolutional side) is based on the ResNet architecture, and the expansive path (deconvolutional side) is based on the U-Net pipeline. Overall, the network performs in an encoder-decoder fashion and is composed of 50 layers (ResNet 50). Our Decoder architecture is explained in Table 6.

Table 6. Decoder Architecture

<i>Layer Name</i>	<i>Kernel</i>	<i>Output Size & No of Filters</i>	<i>Layer Name</i>	<i>Kernel</i>	<i>Output Size & No of Filters</i>
<i>U1</i>	2×2	$16 \times 16 \times 2048$	<i>D6</i>	3×3	$64 \times 64 \times 64$
<i>D1</i>	3×3	$16 \times 16 \times 256$	<i>U4</i>	2×2	$128 \times 128 \times 64$
<i>D2</i>	3×3	$16 \times 16 \times 256$	<i>D7</i>	3×3	$128 \times 128 \times 32$
<i>U2</i>	2×2	$32 \times 32 \times 256$	<i>D8</i>	3×3	$128 \times 128 \times 32$
<i>D3</i>	3×3	$32 \times 32 \times 128$	<i>U5</i>	2×2	$256 \times 256 \times 32$
<i>D4</i>	3×3	$32 \times 32 \times 128$	<i>D9</i>	3×3	$256 \times 256 \times 16$
<i>U3</i>	2×2	$64 \times 64 \times 128$	<i>D10</i>	3×3	$256 \times 256 \times 16$
<i>D5</i>	3×3	$64 \times 64 \times 64$	<i>Output</i>	1×1	$256 \times 256 \times 1$

In decoder, we have pair of deconvolutional layers, that performs upsampling. A 2×2 filter with a stride of 2 is defined that doubles the incoming dimensions.

Hyperparameters

Hyperparameters were adjustment during the training phase to optimize them to help the network in learning the best features. The final hyperparameters employed in training are listed below in Table 7.

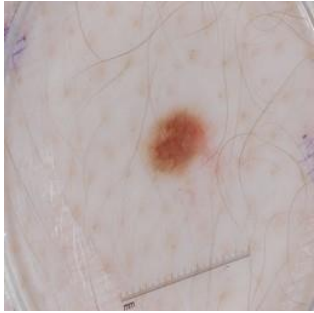
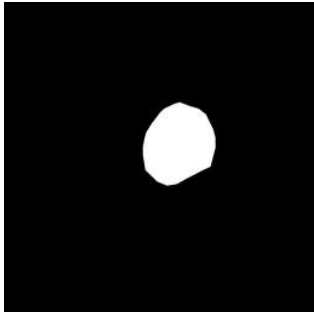

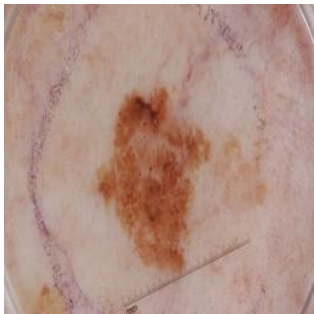
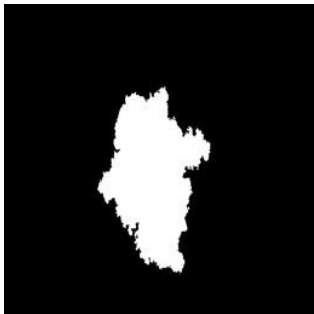

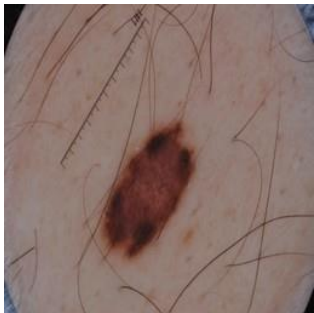
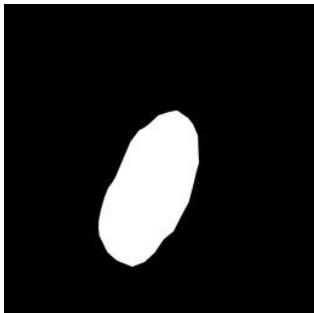

Table 7. Hyperparameters

<i>Name</i>	<i>Value</i>
<i>Input Size</i>	$256 \times 256 \times 3$
<i>Batch Size</i>	16
<i>Learning rate</i>	$1e^{-3}$
<i>Optimizer</i>	<i>Adam</i>
<i>Epoch</i>	100
<i>Loss Function</i>	<i>binary_crossentropy</i>

Segmentation Results

We trained our model named “ResUNet” on ISIC 2017 dataset. A comparison of the actual labels and the predicted labels is given in Table 8. The visualization between predicted label and the actual label show that the proposed model outperforms in the sense that actual labels have hair like structures reflected in their masks. Our model predicted smooth mask because we have preprocessed images before giving to neural network.

Table 8. Comparison of actual and predicted labels.

Image Name	Image	Actual Label	Predicted Label
ISIC_0012095			
ISIC_0012199			
ISIC_0012092			

Training Accuracy Graph

Our model is trained for 100 epochs. Parameters are fine-tuned for increasing performance of our model. Model is early stopped with a patience of 10. For early stopping, validation loss is defined as the quantity to be monitored while training. We plotted a graph between model training accuracy and validation accuracy with epochs on x-axis and accuracy on y-axis.

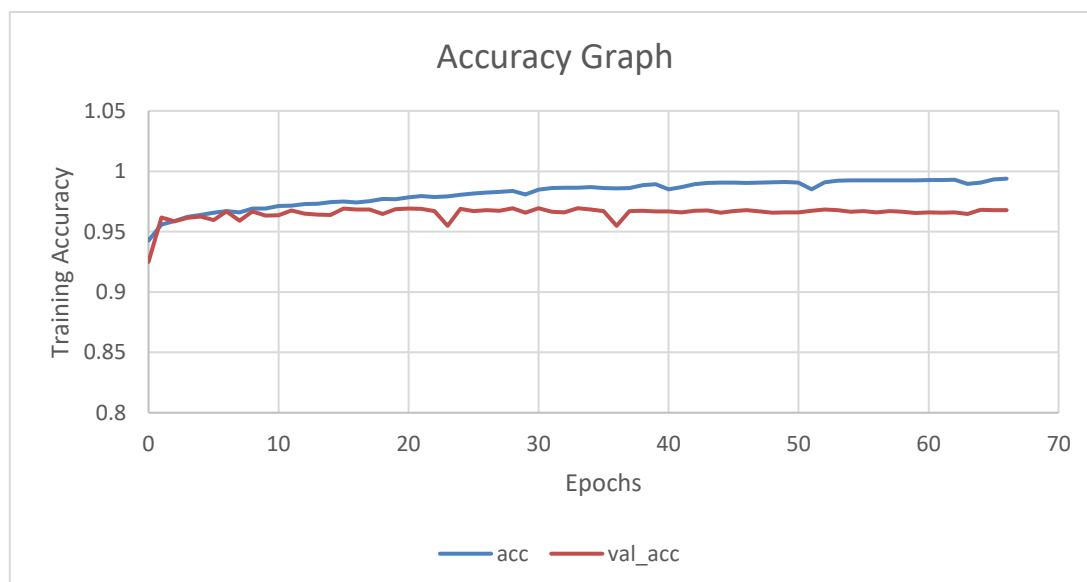


Figure 20. Model Accuracy Graph

Training Loss Graph

Model loss graph is also plotted along with accuracy graph with training loss and validation loss on y-axis and epochs on x-axis.

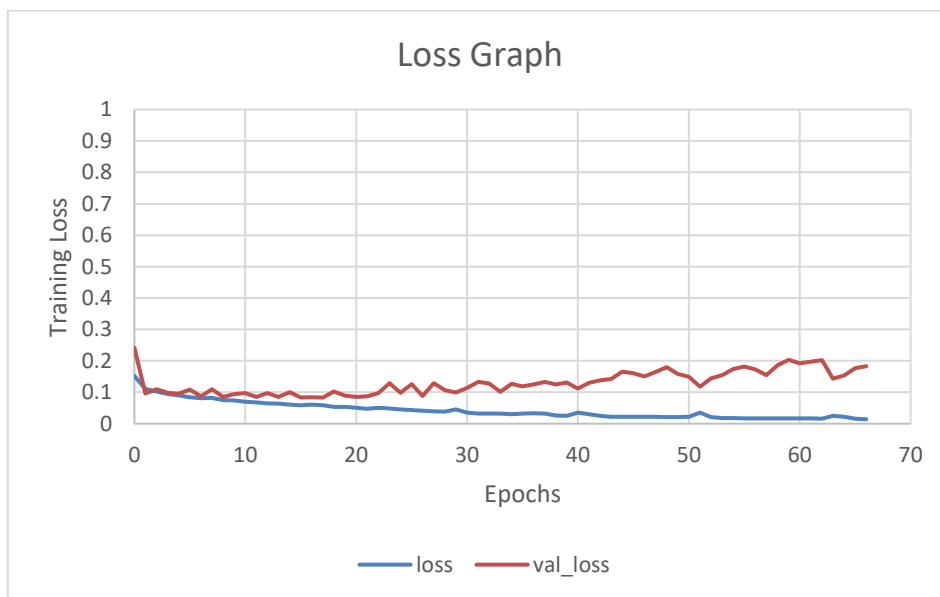


Figure 21. Model Loss graph

Receiver Operator Characteristics (ROC) Curve

In order to visualize the performance of our model, Receiver Operator Characteristics (ROC) curve or Area Under the Curve (AUC) is plotted. It defines how much the network can define between classes.

Higher the AUC , better is the model for predicting 0s as 0s and 1s as 1s.

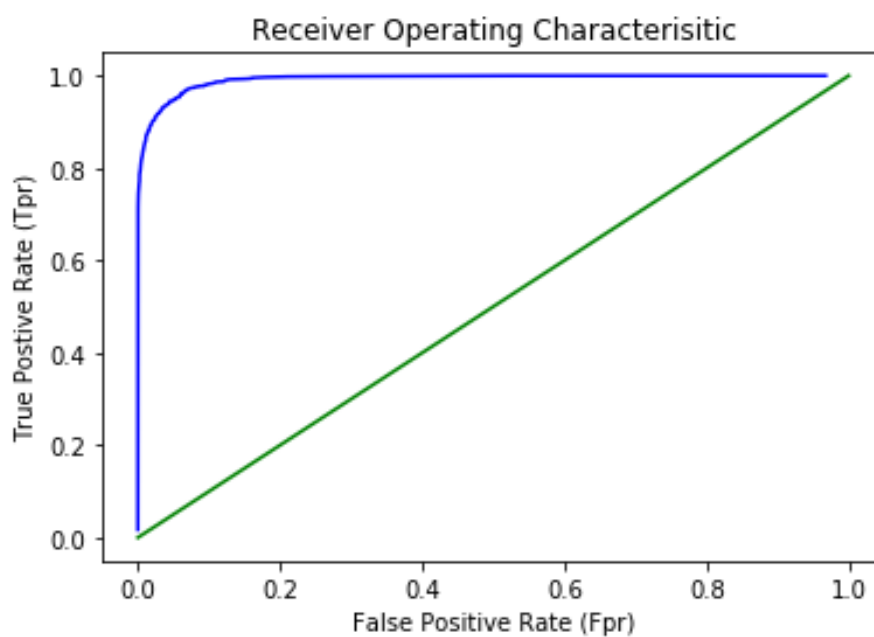


Figure 22. Receiver Operator Characterization Curve

Results Benchmarking on ISIC 2017 Dataset

We participated in ISIC 2017 challenge named “SKIN LESION ANALYSIS TOWARDS MELANOMA DETECTION”. We compare our results with the top 5 submissions from leaderboard. We outperform them and achieved higher score in terms of Jaccard index. Table 9 explains top five submission and their scores in terms of Jaccard index.

Table 9. Results Benchmarking with top ranked participant on leaderboard (ISIC 2017

Sr No	Authors	Model	Score
1	Yading Yuan et al.	CDNN	0.765
2	Matt Berseth et al.	U-Net	0.762
3	Popleyi et al.	FCN	0.760
4	Euijoon Ahn et al.	ResNet	0.758
5	Afonso Menegola et al.	VGG16	0.754
6	Proposed Method	ResUNet	0.772

Dataset)

Results Benchmarking on PH² Dataset

For evaluation purpose, we have further tested our model on PH² dataset to check either our model has performed well on unseen dataset. We compared our results with existing architectures and our model(ResUnet50) has outperformed other architectures in terms of Jaccard index and Dice coefficient. Results are shown in Table 10.

Table 10. Results Benchmarking with existing architectures on PH² dataset

Sr No	Methods	Jaccard Index	Dice Coefficient
1	FCN-16s	0.802	0.881
2	DeeplabV3+	0.814	0.890
3	Mask-RCNN	0.830	0.904
4	Multi-Stage FCN	-	0.906
5	SSLS	-	0.916
6	ResUNet (Proposed)	0.854	0.924

Conclusion and Discussions

CHAPTER 5: Conclusion and Discussions

The International Skin Imaging Collaboration (ISIC) archive hosted a challenge named “*Skin Lesion Analysis Towards Melanoma Detection*” at International Biomedical Imaging Symposium (ISBI) 2017. Basically, this challenge is to develop a diagnosis system that detect region of interest (ROI) from the images and classify them a benign or a malignant tumor. This challenge is divided into three parts; Skin Lesion Segmentation , Lesion Dermoscopic Feature Extraction and Lesion Classification. ISIC provides an environment , that helps researchers for comparing results with other participants by submitting their submission on a platform. This challenge involved 593 submissions, 81 pre-submissions and , 41 finalized submissions. All these arrangements make this challenge the largest comparative study in the associated field.

Skin lesion segmentation has a vital importance for developing a computer assisted diagnosis system. Accurate segmentation is the first step for a proper diagnosis and detection of skin related diseases. Skin lesion is a significant area of interest for prevention and early diagnosis of skin cancer. Although there are several existing state of the art method that provides solution to this problem but still there is a room for further improvement in segmentation techniques. Further improvement is needed for using these techniques to detect skin cancer in a clinical setting. This article proposes a technique that applies some pre-processing on images and achieved promising results compared to the existing methods in the literature.

Since improving segmentation results is a challenging task. This paper proposes a method based on deep learning that automatically segments true part of the skin lesion. Experimental results depict the performance and excellence of our proposed model in extracting skin lesion from the images.

Future Aspects

- Developing a complete diagnosis system, that can perfectly segment skin images and classify them as a malignant or non-malignant tumor.
- In future, focused studies are required to use this system in a clinical setting to help dermatologist for an accurate and precise examination of skin cancer.

- With more data in future, can increase the performance of the proposed convolutional neural network (CNN).

REFERENCES

- [1] “Epidemiology of Malignant Melanoma - Google Books.”
- [2] R. B. Oliveira, M. E. Filho, Z. Ma, J. P. Papa, A. S. Pereira, and J. M. R. S. Tavares, “Computational methods for the image segmentation of pigmented skin lesions: A review,” *Comput. Methods Programs Biomed.*, vol. 131, pp. 127–141, 2016.
- [3] “Skin Cancer | Skin Cancer Facts | Common Skin Cancer Types.” [Online]. Available: <https://www.cancer.org/content/cancer/en/cancer/skin-cancer.html>. [Accessed: 11-Sep-2019].
- [4] N. H. Matthews, W.-Q. Li, A. A. Qureshi, M. A. Weinstock, and E. Cho, “Epidemiology of Melano[1] N. H. Matthews, W.-Q. Li, A. A. Qureshi, M. A. Weinstock, and E. Cho, ‘Epidemiology of Melanoma,’ in *Cutaneous Melanoma: Etiology and Therapy*, Codon Publications, 2017, pp. 3–22.ma,” in *Cutaneous Melanoma: Etiology and Therapy*, Codon Publications, 2017, pp. 3–22.
- [5] “Worldwide cancer statistics | Cancer Research UK.” [Online]. Available: <https://www.cancerresearchuk.org/health-professional/cancer-statistics/worldwide-cancer>.
- [6] N. C. F. Codella *et al.*, “Skin Lesion Analysis Toward Melanoma Detection: A Challenge at the 2017 International Symposium on Biomedical Imaging (ISBI), Hosted by the International Skin Imaging Collaboration (ISIC),” Oct. 2017.
- [7] “Covalic.” <https://challenge.kitware.com/#phase/584b0afacad3a51cc66c8e24>. [Accessed: 02-Oct-2019].
- [8] “Melanoma Statistics - Melanoma Research Alliance.”
- [9] J. Ferlay *et al.*, “Estimating the global cancer incidence and mortality in 2018: GLOBOCAN sources and methods,” *International Journal of Cancer*, vol. 144, no. 8. Wiley-Liss Inc., pp. 1941–1953, 15-Apr-2019.
- [10] “Melanoma: Statistics | Cancer.Net.”
- [11] “Encyclopedia of Cancer and Society - Graham A. Colditz - Google Books.”
- [12] E. Ruocco, G. Argenziano, G. Pellacani, and S. Seidenari, “Noninvasive imaging of skin

- tumors.,” *Dermatol. Surg.*, vol. 30, no. 2 Pt 2, pp. 301–10, Feb. 2004.
- [13] L. Smith and S. Macneil, “State of the art in non-invasive imaging of cutaneous melanoma.,” *Skin Res. Technol.*, vol. 17, no. 3, pp. 257–69, Aug. 2011.
- [14] A. Wong, J. Scharcanski, and P. Fieguth, “Automatic skin lesion segmentation via iterative stochastic region merging,” *IEEE Trans. Inf. Technol. Biomed.*, vol. 15, no. 6, pp. 929–936, Nov. 2011.
- [15] M. E. Celebi and G. Schaefer, Eds., *Color Medical Image Analysis*, vol. 6. Dordrecht: Springer Netherlands, 2013.
- [16] M. Ramezani, A. Karimian, and P. Moallem, “Automatic Detection of Malignant Melanoma using Macroscopic Images.,” *J. Med. Signals Sens.*, vol. 4, no. 4, pp. 281–90, Oct. 2014.
- [17] M. Silveira *et al.*, “Comparison of Segmentation Methods for Melanoma Diagnosis in Dermoscopy Images,” *IEEE J. Sel. Top. Signal Process.*, vol. 3, no. 1, 2009.
- [18] M. E. Yüksel and M. Borlu, “Accurate segmentation of dermoscopic images by image thresholding based on type-2 fuzzy logic,” *IEEE Trans. Fuzzy Syst.*, vol. 17, no. 4, pp. 976–982, 2009.
- [19] H. Zhou *et al.*, “Skin lesion segmentation using an improved snake model.,” *Conf. Proc. ... Annu. Int. Conf. IEEE Eng. Med. Biol. Soc. IEEE Eng. Med. Biol. Soc. Annu. Conf.*, vol. 2010, pp. 1974–7, 2010.
- [20] G. Argenziano and H. P. Soyer, “Dermoscopy of pigmented skin lesions--a valuable tool for early diagnosis of melanoma.,” *Lancet. Oncol.*, vol. 2, no. 7, pp. 443–9, Jul. 2001.
- [21] N. Codella *et al.*, “Deep Learning Ensembles for Melanoma Recognition in Dermoscopy Images,” Oct. 2016.
- [22] C. Barata, M. Ruela, M. Francisco, T. Mendonca, and J. S. Marques, “Two systems for the detection of melanomas in dermoscopy images using texture and color features,” *IEEE Syst. J.*, vol. 8, no. 3, pp. 965–979, 2014.
- [23] M. E. Celebi *et al.*, “Border detection in dermoscopy images using statistical region merging,” *Ski. Res. Technol.*, vol. 14, no. 3, pp. 347–353, Aug. 2008.
- [24] G. Schaefer, M. I. Rajab, M. E. Celebi, and H. Iyatomi, “Colour and contrast enhancement for improved skin lesion segmentation.,” *Comput. Med. Imaging Graph.*,

- vol. 35, no. 2, pp. 99–104, Mar. 2011.
- [25] T. Lee, V. Ng, R. Gallagher, A. Coldman, and D. McLean, “DullRazor: a software approach to hair removal from images.,” *Comput. Biol. Med.*, vol. 27, no. 6, pp. 533–43, Nov. 1997.
- [26] “Digital Image Processing and Analysis - Chanda Bhabatosh, majumder Dwijesh Dutta - Google Books.”
- [27] Q. Abbas, I. F. Garcia, M. Emre Celebi, W. Ahmad, and Q. Mushtaq, “A perceptually oriented method for contrast enhancement and segmentation of dermoscopy images.,” *Skin Res. Technol.*, vol. 19, no. 1, pp. e490-7, Feb. 2013.
- [28] M. Emre Celebi, Y. Alp Aslandogan, W. V Stoecker, H. Iyatomi, H. Oka, and X. Chen, “Unsupervised border detection in dermoscopy images.,” *Skin Res. Technol.*, vol. 13, no. 4, pp. 454–62, Nov. 2007.
- [29] J. Glaister, R. Amelard, A. Wong, and D. A. Clausi, “MSIM: Multistage illumination modeling of dermatological photographs for illumination-corrected skin lesion analysis,” *IEEE Trans. Biomed. Eng.*, vol. 60, no. 7, pp. 1873–1883, 2013.
- [30] M. E. Celebi, H. Iyatomi, and G. Schaefer, “Contrast enhancement in dermoscopy images by maximizing a histogram bimodality measure,” in *Proceedings - International Conference on Image Processing, ICIP*, 2009, pp. 2601–2604.
- [31] P. G. Cavalcanti, J. Scharcanski, and C. B. O. Lopes, “Shading attenuation in human skin color images,” in *Lecture Notes in Computer Science (including subseries Lecture Notes in Artificial Intelligence and Lecture Notes in Bioinformatics)*, 2010, vol. 6453 LNCS, no. PART 1, pp. 190–198.
- [32] M. E. Celebi *et al.*, “A methodological approach to the classification of dermoscopy images,” *Comput. Med. Imaging Graph.*, vol. 31, no. 6, pp. 362–373, Sep. 2007.
- [33] C. A. Z. Barcelos and V. B. Pires, “An automatic based nonlinear diffusion equations scheme for skin lesion segmentation,” *Appl. Math. Comput.*, vol. 215, no. 1, pp. 251–261, Sep. 2009.
- [34] T. F. Chan, B. Yezrielev Sandberg, and L. A. Vese, “Active contours without edges for vector-valued images,” *J. Vis. Commun. Image Represent.*, vol. 11, no. 2, pp. 130–141, 2000.

- [35] H. Iyatomi, M. E. Celebi, H. Oka, and M. Tanaka, "An Internet-based melanoma screening system with acral volar lesion support," in *2008 30th Annual International Conference of the IEEE Engineering in Medicine and Biology Society*, 2008, pp. 5156–5159.
- [36] R. Mishra and O. Daescu, "Deep learning for skin lesion segmentation," in *Proceedings - 2017 IEEE International Conference on Bioinformatics and Biomedicine, BIBM 2017*, 2017, vol. 2017–January, pp. 1189–1194.
- [37] M. H. Jafari *et al.*, "Skin lesion segmentation in clinical images using deep learning," in *Proceedings - International Conference on Pattern Recognition*, 2016, vol. 0, pp. 337–342.
- [38] Y. Li and L. Shen, "Skin lesion analysis towards melanoma detection using deep learning network," *Sensors (Switzerland)*, vol. 18, no. 2, Feb. 2018.
- [39] Y. Yuan and Y. C. Lo, "Improving Dermoscopic Image Segmentation With Enhanced Convolutional-Deconvolutional Networks," *IEEE J. Biomed. Heal. Informatics*, vol. 23, no. 2, pp. 519–526, Mar. 2019.
- [40] F. Y. Xie, S. Y. Qin, Z. G. Jiang, and R. S. Meng, "PDE-based unsupervised repair of hair-occluded information in dermoscopy images of melanoma," *Comput. Med. Imaging Graph.*, vol. 33, no. 4, pp. 275–282, Jun. 2009.
- [41] H. Castillejos, V. Ponomaryov, L. Nino-De-Rivera, and V. Golikov, "Wavelet transform fuzzy algorithms for dermoscopic image segmentation," *Comput. Math. Methods Med.*, vol. 2012, 2012.
- [42] D. D. Gómez, C. Butakoff, B. K. Ersbøll, and W. Stoecker, "Independent histogram pursuit for segmentation of skin lesions," *IEEE Trans. Biomed. Eng.*, vol. 55, no. 1, pp. 157–161, Jan. 2008.
- [43] Z. Ma and J. M. R. S. Tavares, "A Novel Approach to Segment Skin Lesions in Dermoscopic Images Based on a Deformable Model," *IEEE J. Biomed. Heal. Informatics*, vol. 20, no. 2, pp. 615–23, Mar. 2016.
- [44] Q. Abbas, M. E. Celebi, I. Fondón García, and M. Rashid, "Lesion border detection in dermoscopy images using dynamic programming," *Skin Res. Technol.*, vol. 17, no. 1, pp. 91–100, Feb. 2011.

- [45] Q. Abbas, M. E. Celebi, and I. Fondón García, “Skin tumor area extraction using an improved dynamic programming approach.,” *Skin Res. Technol.*, vol. 18, no. 2, pp. 133–42, May 2012.
- [46] “Practical genetic algorithms,” *Choice Rev. Online*, vol. 35, no. 10, pp. 35-5711-35–5711, Jun. 1998.
- [47] J. R. Koza, “Genetic programming as a means for programming computers by natural selection,” *Stat. Comput.*, vol. 4, no. 2, pp. 87–112, Jun. 1994.
- [48] J. Maeda, A. Kawano, S. Yamauchi, Y. Suzuki, A. R. S. Marçal, and T. Mendonça, “Perceptual image segmentation using fuzzy-based hierarchical algorithm and its application to images dermoscopy,” in *SMCia/08 - Proceedings of the 2008 IEEE Conference on Soft Computing on Industrial Applications*, 2008, pp. 66–71.
- [49] A. Masood and A. A. Al-Jumaily, “Fuzzy C Mean Thresholding based Level Set for Automated Segmentation of Skin Lesions,” *J. Signal Inf. Process.*, vol. 4, pp. 66–71, 2013.
- [50] P. R. Tamilselvi, “Analysis of Image Segmentation Techniques for Medical Images,” *Int. Conf. Emerg. Res. Comput. Information, Commun. Appl.*, vol. 2, no. 3, pp. 73–76, 2014.
- [51] O. Ronneberger, P. Fischer, and T. Brox, “2015-U-Net,” pp. 1–8.
- [52] D. P. Kingma and J. Ba, “Adam: A Method for Stochastic Optimization,” Dec. 2014.
- [53] “MadryLab/mnist_challenge: A challenge to explore adversarial robustness of neural networks on MNIST.”

Turnitin Originality Report	
Processed on: 18-Dec-2019 01:14 PKT ID: 1168613382 Word Count: 6507 Submitted: 8	
Melanoma thesis By Kashan Zafar	
Similarity Index 10%	Similarity by Source Internet Sources: 5% Publications: 5% Student Papers: 6%

2% match (student papers from 29-Mar-2019) Submitted to University of Dundee on 2019-03-29
1% match (student papers from 15-Mar-2019) Submitted to University of Computer Studies on 2019-03-15
1% match (publications) Rashika Mishra, Ovidiu Daescu. "Deep learning for skin lesion segmentation", 2017 IEEE International Conference on Bioinformatics and Biomedicine (BIBM), 2017
1% match (publications) Oliveira, Roberta B., Mercedes E. Filho, Zhen Ma, João P. Papa, Aledir S. Pereira, and João Manuel R.S. Tavares. "Computational methods for the image segmentation of pigmented skin lesions: A review", Computer Methods and Programs in Biomedicine, 2016.
< 1% match (publications) "Advances in Multimedia Information Processing – PCM 2018", Springer Nature America, Inc, 2018
< 1% match (Internet from 23-Jun-2019) https://arxiv.org/pdf/1602.09046.pdf
< 1% match (publications) Muhammad Ammar, Sajid Gul Khawaja, Abeera Atif, Muhammad Usman Akram, Muntaha Sakeena. "Learning Based Segmentation of Skin Lesion from Dermoscopic Images", 2018 IEEE 20th International Conference on e-Health Networking, Applications and Services (Healthcom), 2018
< 1% match (Internet from 17-Jan-2019) https://link.springer.com/chapter/10.1007/978-3-319-94544-6_6
< 1% match (Internet from 18-Jan-2019) http://www.healthcenterrx.com/2017/06/05/skin-cancer-awareness/
< 1% match (student papers from 11-Dec-2019) Submitted to Higher Education Commission Pakistan on 2019-12-11
< 1% match (publications) Neda Zamani Tajeddin, Babak Mohammadzadeh Asi. "A general algorithm for automatic lesion segmentation in dermoscopy images", 2016 23rd Iranian Conference on Biomedical Engineering and 2016 1st International Iranian Conference on Biomedical Engineering (ICBME), 2016
< 1% match (publications) Ruela, Margarida, Catarina Barata, Jorge S. Marques, and Jorge Rozeira. "A system for the detection of melanomas in dermoscopy images using shape and symmetry features", Computer Methods in Biomechanics and Biomedical Engineering Imaging & Visualization, 2015.
< 1% match (Internet from 04-Dec-2019) https://www.48hours.ai/files/AUC.pdf
< 1% match () https://repositorio-aberto.up.pt/handle/10216/79960
< 1% match (publications) Sameena Pathan, K. Gopalakrishna Prabhu, P.C. Siddalingaswamy. "Techniques and algorithms for computer aided diagnosis of pigmented skin lesions—A review", Biomedical Signal Processing and Control, 2018
< 1% match () https://www.hal.inserm.fr/inserm-00608891
< 1% match (publications) "Information Processing in Medical Imaging", Springer Science and Business Media LLC, 2019
< 1% match (student papers from 19-Aug-2019) Submitted to Coventry University on 2019-08-19
< 1% match (student papers from 13-Sep-2018) Submitted to University of Warwick on 2018-09-13
< 1% match () https://eprints.qut.edu.au/53295/
< 1% match (Internet from 12-Dec-2019)